Biochemical and Biophysical Research Communications 424 (2012) 629–634

Contents lists available at SciVerse ScienceDirect

Biochemical and Biophysical Research Communications

journal homepage: www.elsevier.com/locate/ybbrc

Isolation and characterizations of oxalate-binding proteins in the kidney

Piyachat Roop-ngam, Sakdithep Chaiyarit, Nutkridta Pongsakul, Visith Thongboonkerd *

Medical Proteomics Unit, Office for Research and Development, Faculty of Medicine Siriraj Hospital, and Center for Research in Complex Systems Science, Mahidol University, Bangkok, Thailand

ARTICLE INFO

Article history:
Received 4 July 2012
Available online 14 July 2012

Keywords:
Kidney stone
Nephrolithiasis
Oxalate
Oxalate-binding
Proteins
Proteomics

ABSTRACT

Oxalate-binding proteins are thought to serve as potential modulators of kidney stone formation. However, only few oxalate-binding proteins have been identified from previous studies. Our present study, therefore, aimed for large-scale identification of oxalate-binding proteins in porcine kidney using an oxalate-affinity column containing oxalate-conjugated EAH Sepharose 4B beads for purification followed by two-dimensional gel electrophoresis (2-DE) to resolve the recovered proteins. Comparing with those obtained from the controlled column containing uncoupled EAH-Sepharose 4B (to subtract the background of non-specific bindings), a total of 38 protein spots were defined as oxalate-binding proteins. These protein spots were successfully identified by quadrupole time-of-flight mass spectrometry (MS) and/or tandem MS (MS/MS) as 26 unique proteins, including several nuclear proteins, mitochondrial proteins, oxidative stress regulatory proteins, metabolic enzymes and others. Identification of oxalate-binding domain using the PRATT tool revealed "*L-x(3,5)-R-x(2)-[AGILPV]*" as a functional domain responsible for oxalate-binding in 25 of 26 (96%) unique identified proteins. We report herein, for the first time, large-scale identification and characterizations of oxalate-binding proteins in the kidney. The presence of positively charged arginine residue in the middle of this functional domain suggested its significance for binding to the negatively charged oxalate. These data will enhance future stone research, particularly on stone modulators.

1. Introduction

Recently, kidney stone disease has been investigated extensively at the molecular level. Among all stone types, calcium oxalate (CaOx) is the most common inorganic matrix found in kidney stones [1]. In addition to inorganic matrix, organic compounds, particularly proteins, are also found in kidney stones [2]. Many previous studies have focused on identification of CaOx kidney stone modulators and proposed that some of the calcium- and oxalate-binding proteins may serve as the stone modulators [3–6]. From these efforts, some of calcium-binding proteins that have inhibitory activity against CaOx crystal growth and aggregation have been successfully identified [7–12]. On the other hand, a much fewer number of previous studies have attempted to characterize oxalate-binding proteins, which also have potential role in kidney stone disease [6]. A number of oxalate-binding proteins have been isolated from kidney homogenate and stone matrix [6]. Among these, only histone has been successfully identified and characterized [13]. This under-investigation is probably due to a lack of simple method for isolation of oxalate-binding proteins in the past.

We have recently developed an oxalate-affinity chromatographic column for highly efficient and simplified isolation/purification of oxalate-binding proteins [14]. In the present study, our oxalate-affinity chromatographic column containing oxalate-conjugated EAH Sepharose 4B beads was applied to purify oxalate-binding proteins from porcine kidney. The recovered proteins were resolved by 2-DE compared to those recovered from the controlled column containing unconjugated EAH-Sepharose 4B (to subtract the background of non-specific bindings). The oxalate-binding proteins were then identified by Q-TOF MS and/or MS/MS analyses. Finally, the identified proteins were subjected to identification of functional domain responsible for oxalate-binding.

2. Materials and methods

2.1. Preparation of oxalate-affinity chromatographic column

The oxalate-affinity chromatographic column was prepared as we described previously [14]. In principle, oxalic acid was conjugated (through carboxylic groups) to EAH Sepharose 4B (via primary amine groups). Coupling efficacy was determined quantitatively

* Corresponding author. Address: Head of Medical Proteomics Unit, Director of Center for Research in Complex Systems Science (CRCSS), Siriraj Hospital, Mahidol University, 10th Floor Srisawarinthira Building, 2 Prannok Road, Bangkoknoi, Bangkok 10700, Thailand. Fax: +66 2 4195503.
E-mail addresses: vthongbo@yahoo.com, thongboonkerd@dr.com (V. Thongboonkerd).

0006-291X/$ - see front matter © 2012 Elsevier Inc. All rights reserved.
http://dx.doi.org/10.1016/j.bbrc.2012.07.015

by measuring the remaining primary amine groups on EAH-Sepharose 4B beads using a competitive nindydrin assay [14]. For the controlled column, EAH Sepharose 4B beads were treated and processed with similar procedures as for the oxalate-affinity column, but without oxalic acid conjugation.

2.2. Isolation of oxalate-binding proteins from porcine kidney

A porcine kidney was bought from a local fresh poultry market. The tissue was then dissected into thin slices, washed with phosphate buffered saline (PBS), snap frozen in liquid nitrogen and ground into powder using pre-chilled mortar and pestle. Tissue powder was then resuspended in Tris–HCl buffer (pH 6.5). The kidney sample was then centrifuged at 12,000*g*, 4 °C for 5 min to remove the particulate matters. The supernatant was saved and protein concentration was measured by the Bradford method. To isolate oxalate-binding proteins, 3 mg of the recovered porcine kidney proteins was passed through the affinity column with a flow rate of 1 mL/min. Thereafter, the column was first eluted with 20 mL of a binding buffer containing 10 mM 2-morpholinoethanesulfonic acid (MES) in NaOH (pH 6.5), 150 mM NaCl, 2 mM $MgCl_2$, 2 mM $CaCl_2$, and 5 mM KCl to remove non-specific binding proteins. Oxalate-binding proteins were then eluted with 10 mL of an elution buffer containing 10 mM MES in NaOH (pH 6.5), 150 mM NaCl, 2 mM $MgCl_2$, 2 mM $CaCl_2$, 5 mM KCl, 1 M NaCl and 1 mM oxalic acid with 10 fractions (1 mL/fraction). In parallel, 3 mg of the recovered porcine kidney proteins was passed through the controlled column with a flow rate of 1 mL/min. The subsequent steps were exactly the same as for the oxalate-affinity column.

2.3. 2-DE

The eluted protein fractions obtained from the previous step were pooled, desalted by dialysis against 18 MΩ cm (dI) water, and concentrated by lyophilization. The concentrated proteins were then resuspended in 150 μl of rehydration buffer containing 7 M urea, 2 M thiourea, 2% 3-[(3-cholamidopropyl) dimethylammonio]-1-propanesulfonate (CHAPS), 120 mM dithiothreitol (DTT), 2% ampholytes (pH 3–10), 40 mM Tris–HCl, and a trace amount of bromophenol blue. The protein solution was then rehydrated overnight in an Immobiline™ DryStrip, non-linear pH 3–10 (GE Healthcare Bio-Sciences, Uppsala, Sweden). Thereafter, the isoelectric focusing (IEF) was run in Ettan IPGphor III IEF System (GE Healthcare Bio-Sciences) at 20 °C, using a stepwise mode to reach 9083 V h with a current limit of 50 μA/strip. After the IEF completion, proteins on the strip were equilibrated in a buffer containing 6 M urea, 130 mM DTT, 30% glycerol, 112 mM Tris-base, 4% SDS and 0.002% bromophenol blue for 15 min, and then with another buffer containing 6 M urea, 135 mM iodoacetamide, 30% glycerol, 112 mM Tris-base, 4% SDS and 0.002% bromophenol blue for 10 min. For the second dimension, the proteins on the IPG strip were resolved further in 12% polyacrylamide slab gel (8×9.5 cm) using the SE260 Mini-Vertical Electrophoresis Unit (GE Healthcare Bio-Sciences) with a constant voltage of 150 V for 2 h. The resolved protein spots were stained with SYPRO Ruby fluorescence dye (Invitrogen-Molecular Probes; Eugene, OR) and visualized with Typhoon laser scanner (GE Healthcare).

2.4. Spot matching and quantitative intensity analysis

Image Master 2D Platinum (GE Healthcare) software was used for matching and analysis of protein spots in 2-D gels. Parameters used for spot detection were (i) minimal area = 10 pixels; (ii) smooth factor = 2.0; and (iii) saliency = 2.0. A reference gel used for matching the corresponding protein spots among different gels was created from an artificial gel by combining all of the spots presenting in different gels into one image. Background subtraction was performed and the intensity volume of each spot was normalized with total intensity volume (summation of the intensity volumes obtained from all spots within the same 2-D gel). Differentially expressed protein spots were defined as those, which were present only in the sample derived from oxalate-affinity chromatographic column or had intensity levels > 3-fold as compared to those obtained from the controlled column. These differentially expressed protein spots were excised and subjected to in-gel tryptic digestion and identification by Q-TOF MS and MS/MS analyses.

2.5. In-gel tryptic digestion

The excised protein spots were washed twice with 200 μL of 50% acetonitrile (ACN)/25 mM NH_4HCO_3 buffer (pH 8.0) at room temperature for 15 min, and then washed once with 200 μL of 100% ACN. After washing, the solvent was removed, and the gel pieces were dried by a SpeedVac concentrator (Savant; Holbrook, NY) and rehydrated with 10 μL of 1% (w/v) trypsin (Promega; Madison, WI) in 25 mM NH_4HCO_3. After rehydration, the gel pieces were crushed and incubated at 37 °C for at least 16 h. Peptides were subsequently extracted twice with 50 μL of 50% ACN/5% trifluoroacetic acid (TFA); the extracted solutions were then combined and dried with the SpeedVac concentrator. The peptide pellets were resuspended with 10 μL of 0.1% TFA and purified using $ZipTip_{C18}$ (Millipore; Bedford, MA). The peptide solution was drawn up and down in the $ZipTip_{C18}$ 10 times and then washed with 10 μL of 0.1% formic acid by drawing up and expelling the washing solution three times. The peptides were finally eluted with 5 μL of 75% ACN/0.1% formic acid.

2.6. Protein identification by Q-TOF MS and MS/MS analyses

The trypsinized samples were premixed 1:1 with the matrix solution containing 5 mg/mL α-cyano-4-hydroxycinnamic acid (CHCA) in 50% ACN, 0.1% (v/v) TFA and 2% (w/v) ammonium citrate, and deposited onto the 96-well MALDI target plate. The samples were analyzed by Q-TOF Ultima™ mass spectrometer (Micromass; Manchester, UK), which was fully automated with predefined probe motion pattern and the peak intensity threshold for switching over from MS survey scanning to MS/MS, and from one MS/MS to another. Within each sample well, parent ions that met the predefined criteria (any peak within the *m/z* 800–3000 range with intensity above 10 count ± include/exclude list) were selected for CID MS/MS using argon as the collision gas and a mass dependent ± 5 V rolling collision energy until the end of the probe pattern was reached. The MS and MS/MS data were extracted and outputted as the searchable *.txt* and *.pkl* files, respectively, for independent searches using the MASCOT search engine (http://www.matrixscience.com) to query to the NCBI mammalian protein database, assuming that peptides were monoisotopic. Fixed modification was carbamidomethylation at cysteine residues, whereas variable modification was oxidation at methionine residues. Only one missed trypsin cleavage was allowed, and peptide mass tolerances of 100 and 50 ppm were allowed for peptide mass fingerprinting and MS/MS ions search, respectively.

2.7. Identification of oxalate-binding domain

The PRATT tool (http://www.ebi.ac.uk/Tools/pratt/) [15,16], provided by the European Bioinformatics Institute (EBI) was used for characterization of the functional domain in the identified oxalate-binding proteins. All the proteins identified by Q-TOF MS and/or MS/MS analyses (in FASTA format) were altogether aligned and

subjected to the unbiased opened search (without any restrictions or predefined pattern) to define the functional domain responsible for oxalate-binding. After obtaining oxalate-binding domain, sequences of some of the known kidney proteins, which are not the oxalate-binding proteins (see their identities in *Supplementary* Table S1), were submitted to search for such functional domain (to demonstrate the specificity of the identification of the oxalate-binding domain).

3. Results & discussion

The efficacy and specificity of the oxalate-affinity chromatographic column were confirmed in our previous study [14] using the known oxalate-binding protein p62 [17] as the positive control and carbonic anhydrase as the negative control. The extracted porcine kidney proteins were then passed through the oxalate-affinity column to isolate oxalate-binding proteins. In parallel, the proteins were passed through the controlled column to subtract the background of non-specific bindings. The eluate fractions from each column were pooled, and the recovered proteins were resolved by 2-DE and visualized by SYPRO Ruby staining. Using the Image Master 2D Platinum software to match and quantify protein spots across different gels, a total of 38 protein spots were defined as differentially expressed spots between the two groups (Fig. 1). All of these potential oxalate-binding proteins were successfully identified by Q-TOF MS and/or MS/MS analyses as 26 unique proteins. Note that some of them had many isoforms and were thus identified as one unique protein. Details of their identities, identification numbers, identification scores, percentage of sequence coverage (%Cov), numbers of matched peptides, isoelectric points (pI) and molecular weights (MW) are summarized in Table 1.

All the identified proteins were subjected to characterization of oxalate-binding domain using the PRATT tool (http://www.ebi.ac.uk/Tools/pratt/) [15,16], provided by the European Bioinformatics Institute (EBI). The data revealed a domain/pattern "L-x(3,5)-R-x(2)-[AGILPV]" in 25 of 26 (approximately 96%) unique proteins identified by Q-TOF MS and/or MS/MS analyses (Fig. 2). Among these 25 proteins with oxalate-binding domain, 15 proteins had more than one oxalate-binding domain in their sequences, and the greatest number of this domain in each protein was 19, which was found in the sequence of transformation/transcription domain-associated protein isoform 2 (spot #38). Interestingly, the presence of positively charged arginine residue in the middle of this functional domain suggested its significance for binding to the negatively charged oxalate. To demonstrate the specificity of this oxalate-binding domain, sequences of some of the known kidney proteins, which are not oxalate-binding proteins (see their identities in *Supplementary* Table S1), were also submitted to the PRATT tool to search for such functional domain. The data revealed that none of these non-oxalate-binding kidney proteins had the domain "*L-x(3,5)-R-x(2)-[AGILPV]*" in their sequences (*Supplementary* Table S1). These data implicate the specificity of this functional domain, which is responsible for oxalate-binding.

The present study identified histone H2A (spot #14) as one of the nuclear oxalate-binding proteins in porcine kidney, consistent to the data reported in a previous study demonstrating that histone serves as a known oxalate-binding protein in kidney homogenate and stone matrix [13]. These concordant results strengthened that our oxalate-affinity chromatographic column is reliable and effective for isolation and enrichment of oxalate-binding proteins. In previous studies, one third of oxalate-binding proteins have been found in mitochondria of renal cells [6]. There were a number of mitochondrial oxalate-binding proteins identified in this study, including mitochondrial precursor of ATP synthase subunit beta (spot #13), mitochondrial Aacyl-CoA dehydrogenase (spot #19), mitochondrial NADH:ubiquinone oxidoreductase 51 kDa subunit (spot #22), and mitochondrial malate dehydrogenase 2 NAD (spot #24).

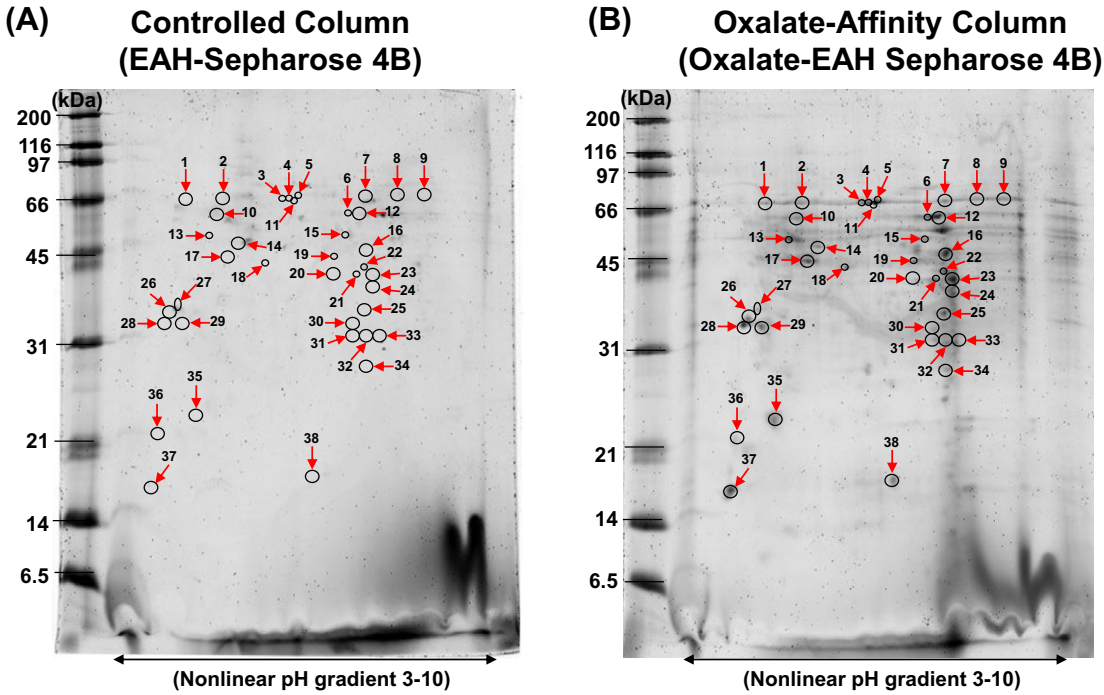

Fig. 1. 2-DE map of oxalate-binding proteins in porcine kidney. Porcine kidney proteins were passed through either controlled column containing EAH-Sepharose 4B beads (A) or oxalate-affinity column containing oxalate-conjugated EAH-Sepharose 4B beads (B). The eluate fractions from each column were pooled and the recovered proteins were resolved by 2-DE, and visualized by SYPRO Ruby staining. Protein spots that were present only in the sample derived from oxalate-affinity chromatographic column or had intensity levels > 3-fold as compared to those obtained from the controlled column were subjected to identification by Q-TOF MS and MS/MS analyses (see details in Table 1).

Table 1
Summary of oxalate-binding proteins in porcine kidney identified by Q-TOF MS and/or MS/MS analyses.

Spot No.	Protein name	NCBI ID	Identified by	Identification scores(MS, MS/MS)	%Cov (MS, MS/MS)	No. of matched peptides (MS, MS/MS)	p*I*	MW (kDa)
1	Albumin	gi|833798	MS, MS/MS	96, 24	20, 2	12, 1	5.92	71.36
2	Albumin	gi|833798	MS, MS/MS	92, 63	26, 6	13, 3	5.92	71.36
3	Albumin	gi|833798	MS, MS/MS	81, 77	22, 4	11, 2	5.92	71.36
4	Albumin	gi|833798	MS, MS/MS	123, 69	33, 4	15, 2	5.92	71.36
5	Albumin	gi|124257959	MS	105, NA	28, NA	14, NA	5.92	71.55
6	Catalase	gi|356460899	MS	114, NA	30, NA	12, NA	6.60	60.18
7	Heterogeneous nuclear ribonucleoprotein M	gi|158455026	MS	65, NA	32, NA	12, NA	9.18	58.37
8	Albumin	gi|833798	MS, MS/MS	103, 159	28, 4	14, 2	5.92	71.36
9	Albumin	gi|833798	MS	90, NA	24, NA	13, NA	5.92	71.36
10	Catalase	gi|356460899	MS	132, NA	36, NA	15, NA	6.60	60.18
11	Albumin	gi|833798	MS, MS/MS	141, 101	34, 6	16, 3	5.92	71.36
12	Catalase	gi|356460899	MS, MS/MS	125, 154	41, 13	14, 15	6.60	60.18
13	ATP synthase subunit beta, mitochondrial precursor	gi|54792127	MS	148, NA	43, NA	16, NA	5.19	56.32
14	Histone H2A.2	gi|31979	MS/MS	NA, 15	NA, 12	NA, 1	9.52	13.64
15	Adenylate kinase 7-like, partial	gi|149592814	MS	74, NA	15, NA	14, NA	7.09	136.97
16	60S ribosomal protein L32-like	gi|296188853	MS/MS	NA, 19	NA, 9	NA, 1	10.58	16.14
17	TNFAIP3-interacting protein 2 isoform 2	gi|239787094	MS	73, NA	34, NA	9, NA	6.12	37.17
18	Sp110 nuclear body protein isoform 6	gi|332815728	MS	78, NA	22, NA	12, NA	9.02	79.66
19	Aacyl-CoA dehydrogenase, mitochondrial	gi|113018	MS/MS	NA, 25	NA, 3	NA, 1	8.63	46.93
20	Fructose-1,6-bisphosphatase	gi|3288991	MS	103, NA	35, NA	11, NA	6.85	36.97
21	Coiled-coil domain-containing protein 40	gi|332263895	MS	74, NA	16, NA	14, NA	5.35	130.47
22	Mitochondrial NADH:ubiquinone oxidoreductase 51 kDa subunit	gi|263364	MS/MS	NA, 7	NA, 7	NA, 1	9.94	14.61
23	p21(CDKN1A)-activated kinase 7	gi|193787901	MS	81, NA	32, NA	11, NA	6.91	65.17
24	Mitochondrial malate dehydrogenase 2, NAD	gi|89574151	MS, MS/MS	109, 30	51, 4	10, 1	8.39	29.92
25	Fibrinogen betaB 1-118	gi|223130	MS/MS	NA, 70	NA, 11	NA, 1	6.17	12.89
26	Adenylosuccinate lyase, partial	gi|334347573	MS	74, NA	25, NA	9, NA	6.36	50.93
27	Transformation/transcription domain-associated protein	gi|344244337	MS	89, NA	11, NA	19, NA	8.30	228.20
28	Uncharacterized protein C3orf77-like	gi|332215705	MS	78, NA	13, NA	18, NA	8.17	192.59
29	Tissue-type plasminogen activator-like	gi|334312618	MS	95, NA	23, NA	11, NA	8.65	65.03
30	Tubulin polymerization-promoting protein family member 3-like isoform 1	gi|332227511	MS	81, NA	46, NA	8, NA	9.18	19.10
31	60S ribosomal protein L32-like	gi|296188853	MS/MS	NA, 19	NA, 9	NA, 1	10.58	16.14
32	CD164 antigen, sialomucin, isoform CRA_c	gi|119568736	MS/MS	NA, 21	NA, 22	NA, 1	12.00	7.27
33	60S ribosomal protein L32-like	gi|296188853	MS/MS	NA, 19	NA, 9	NA, 1	10.58	16.14
34	CD164 antigen, sialomucin, isoform CRA_c	gi|119568736	MS/MS	NA, 20	NA, 22	NA, 1	12.00	7.27
35	CD164 antigen, sialomucin, isoform CRA_c	gi|119568736	MS/MS	NA, 20	NA, 22	NA, 1	12.00	7.27
36	Retinitis pigmentosa GTPase regulator	gi|262050614	MS/MS	NA, 13	NA, 0	NA, 1	8.40	169.82
37	78 kDa glucose-regulated protein, partial	gi|829365	MS/MS	NA, 25	NA, 60	NA, 1	4.66	30.76
38	Transformation/transcription domain-associated protein isoform 2, partial	gi|380799023	MS	76, NA	9, NA	25, NA	8.60	380.25

NCBI = National Center for Biotechnology Information.
%Cov = %Sequence coverage [(number of the matched residues/total number of residues in the entire sequence) × 100%].
NA = Not applicable.

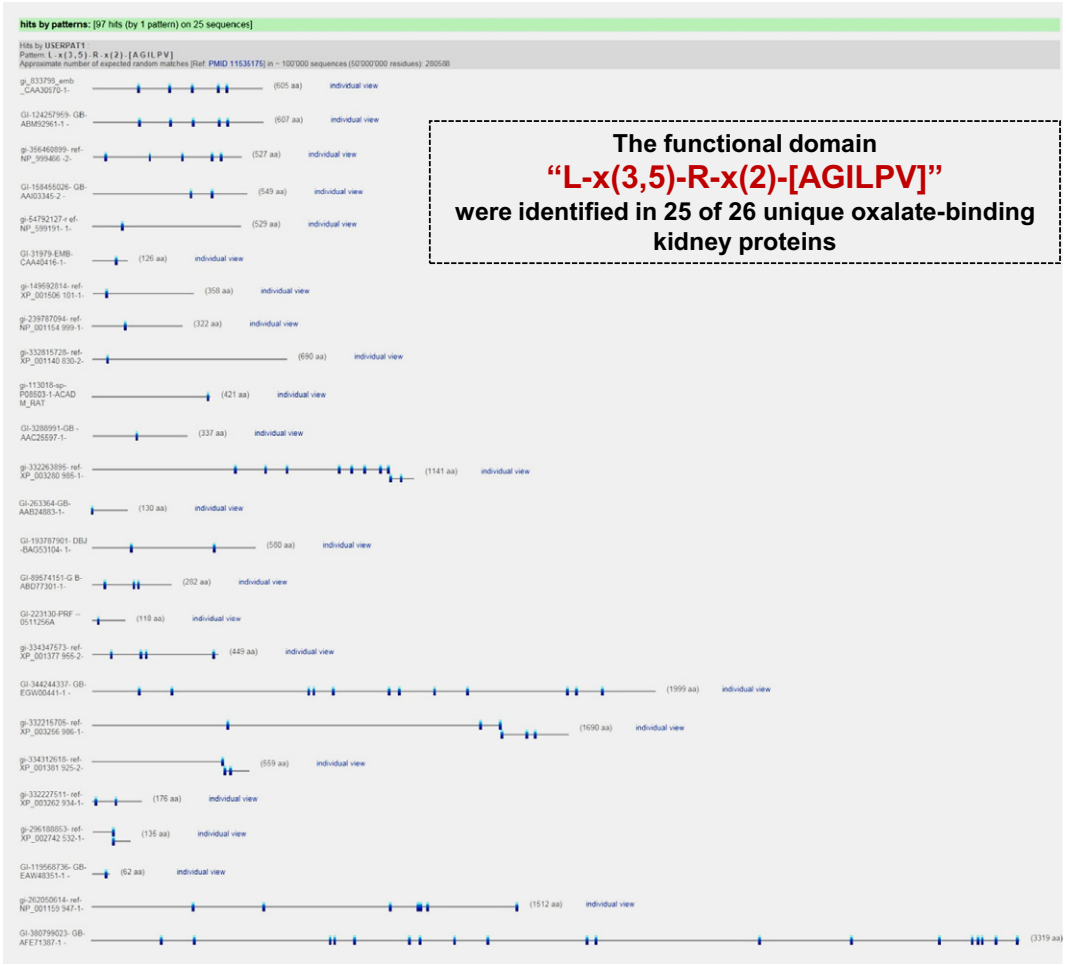

Fig. 2. Identification of oxalate-binding domain. The FASTA format of amino acid sequences of all the identified proteins listed in Table 1 were submitted to the PRATT search tool (http://www.ebi.ac.uk/Tools/pratt/) [15,16]. The data showed the domain "*L-x(3,5)-R-x(2)-[AGILPV]*" in the sequences of 25 of 26 unique proteins identified in Table 1. Among these, 15 had more than one oxalate-binding domain and the greatest number was found in transformation/transcription domain-associated protein isoform 2 (19 sites).

A number of oxidative stress regulatory proteins were identified as oxalate-binding proteins in our present study, including three isoforms of catalase (spots #6, 10, 12), mitochondrial NADH:ubiquinone oxidoreductase 51 kDa subunit (spot #22), and 78 kDa glucose-regulated protein (GRP78) (spot #37). Interestingly, catalase is responsible for catalyzing hydrogen peroxide (H_2O_2) to water (H_2O) and oxygen (O_2) [18]. There is evidence demonstrating that oxalate can induce renal cell injury by lipid peroxidation through reactive oxygen species such as superoxide anion, hydroxyl radicals and hydrogen peroxide. The accumulation of these free radicals is correlated with the decreased level of antioxidant enzymes including catalase, and catalase activity is decreased in rat kidney treated with oxalate [19]. Therefore, the decrease in level and activity of catalase might result to the reduced ability of this enzyme to bind to oxalate. *In vivo* binding of this enzyme to oxalate may be mediated by anti-oxidative processes to protect cell injury from oxidative stress.

Moreover, some metabolic enzymes were identified as oxalate-binding proteins in this study, e.g. malate dehydrogenase (spot #24). This enzyme has been proposed to bind with oxalate since its catalytic subunit binds with malate, which has a molecular structure similar to oxalate. Interestingly, malate dehydrogenase has been also identified in a previous study by Park, et al. [20] using an oxalate-affinity chromatography to purify malate synthase. These findings suggest that the ability of oxalate to bind with this enzyme may be due to the molecular mimicry of oxalate structure to the specific enzyme substrates.

Interestingly, we also identified many forms of albumin (spots #1–5, 8, 9, and 11) and three isoforms of CD164 (sialomucin) (spots #32, 34 and 35) as the oxalate-binding proteins in porcine kidney. Albumin is widely known as a sticky protein that can bind non-specifically to other proteins and various surfaces, whereas sialomucin has been reported as the secreted or membrane-associated mucin that can act as an adhesion receptor [21,22]. By their properties, it might be postulated that these two proteins could bind non-specifically to the oxalate-affinity column. However, the negative identification of the oxalate-binding domain in the non-oxalate-binding kidney proteins strengthened that albumin and sialomucin were really the oxalate-binding proteins based on the oxalate-binding domain found in their sequences.

In summary, several oxalate-binding proteins were identified from porcine kidney in our present study by a combination of oxalate-affinity purification and proteomics approach. Sequence analysis revealed that almost all of these identified proteins had the oxalate-binding domain "*L-x(3,5)-R-x(2)-[AGILPV]*". These data offer many opportunities for further investigations to address functional significance of these oxalate-binding proteins in renal physiology and pathogenic mechanisms of kidney stone disease.

Acknowledgments

This study was supported by Office of the Higher Education Commission and Mahidol University under the National Research Universities Initiative, and the Thailand Research Fund (RTA5380005 to VT). VT is also supported by "Chalermphrakiat" Grant, Faculty of Medicine Siriraj Hospital.

Appendix A. Supplementary data

Supplementary data associated with this article can be found, in the online version, at http://dx.doi.org/10.1016/j.bbrc.2012.07.015.

References

[1] G. Schubert, Stone analysis, Urol. Res. 34 (2006) 146–150.
[2] F.L. Coe, J.H. Parks, J.R. Asplin, The pathogenesis and treatment of kidney stones, N. Engl. J. Med. 327 (1992) 1141–1152.
[3] R.C. Walton, J.P. Kavanagh, B.R. Heywood, P.N. Rao, The association of different urinary proteins with calcium oxalate hydromorphs. Evidence for non-specific interactions, Biochim. Biophys. Acta 1723 (2005) 175–183.
[4] R. Selvam, P. Kalaiselvi, A novel basic protein from human kidney which inhibits calcium oxalate crystal growth, BJU. Int. 86 (2000) 7–13.
[5] B. Hess, Y. Nakagawa, F.L. Coe, Inhibition of calcium oxalate monohydrate crystal aggregation by urine proteins, Am. J. Physiol. 257 (1989) F99–106.
[6] R. Selvam, P. Kalaiselvi, Oxalate binding proteins in calcium oxalate nephrolithiasis, Urol. Res. 31 (2003) 242–256.
[7] J.C. Lieske, S. Deganello, Nucleation, adhesion, and internalization of calcium-containing urinary crystals by renal cells, J. Am. Soc. Nephrol. 10 (Suppl. 14) (1999) S422–S429.
[8] V. Kumar, G. Farell, J.C. Lieske, Whole urinary proteins coat calcium oxalate monohydrate crystals to greatly decrease their adhesion to renal cells, J. Urol. 170 (2003) 221–225.
[9] S. Chutipongtanate, Y. Nakagawa, S. Sritippayawan, J. Pittayamateekul, P. Parichatikanond, B.R. Westley, F.E. May, P. Malasit, V. Thongboonkerd, Identification of human urinary trefoil factor 1 as a novel calcium oxalate crystal growth inhibitor, J. Clin. Invest. 115 (2005) 3613–3622.
[10] P.K. Grover, L.A. Thurgood, R.L. Ryall, Effect of urine fractionation on attachment of calcium oxalate crystals to renal epithelial cells: implications for studying renal calculogenesis, Am. J. Physiol. Renal Physiol. 292 (2007) F1396–F1403.
[11] V. Thongboonkerd, S. Chutipongtanate, T. Semangoen, P. Malasit, Urinary trefoil factor 1 is a novel potent inhibitor of calcium oxalate crystal growth and aggregation, J. Urol. 179 (2008) 1615–1619.
[12] P.K. Grover, L.A. Thurgood, T. Wang, R.L. Ryall, The effects of intracrystalline and surface-bound proteins on the attachment of calcium oxalate monohydrate crystals to renal cells in undiluted human urine, BJU. Int. 105 (2010) 708–715.
[13] P. Latha, P. Kalaiselvi, P. Varalakshmi, G. Rameshkumar, Characterization of histone (H1B) oxalate binding protein in experimental urolithiasis and bioinformatics approach to study its oxalate interaction, Biochem. Biophys. Res. Commun. 345 (2006) 345–354.
[14] P. Roop-ngam, V. Thongboonkerd, Development of an oxalate-affinity chromatographic column to isolate oxalate-binding proteins, Anal. Methods 2 (2010) 1051–1055.
[15] I. Jonassen, Efficient discovery of conserved patterns using a pattern graph, Comput. Appl. Biosci. 13 (1997) 509–522.
[16] I. Jonassen, J.F. Collins, D.G. Higgins, Finding flexible patterns in unaligned protein sequences, Protein Sci. 4 (1995) 1587–1595.
[17] P. Sivakamasundari, P. Kalaiselvi, R. Sakthivel, R. Selvam, P. Varalakshmi, Nuclear pore complex oxalate binding protein p62: expression in different kidney disorders, Clin. Chim. Acta 347 (2004) 111–119.
[18] T. Henzler, E. Steudle, Transport and metabolic degradation of hydrogen peroxide in *Chara corallina*: model calculations and measurements with the pressure probe suggest transport of H(2)O(2) across water channels, J. Exp. Bot. 51 (2000) 2053–2066.
[19] S. Thamilselvan, K.J. Byer, R.L. Hackett, S.R. Khan, Free radical scavengers, catalase and superoxide dismutase provide protection from oxalate-associated injury to LLC-PK1 and MDCK cells, J. Urol. 164 (2000) 224–229.
[20] J.B. Park, H.Z. Chae, Y.S. Kim, Purification and characterization of malate synthase from *Acinetobacter calcoaceticus* grown on malonate, Korean Biochem. J. 19 (1986) 235–241.
[21] S.M. Watt, H.J. Buhring, I. Rappold, J.Y. Chan, J. Lee-Prudhoe, T. Jones, A.C. Zannettino, P.J. Simmons, R. Doyonnas, D. Sheer, L.H. Butler, CD164, a novel sialomucin on CD34(+) and erythroid subsets, is located on human chromosome 6q21, Blood 92 (1998) 849–866.
[22] S. Forde, B.J. Tye, S.E. Newey, M. Roubelakis, J. Smythe, C.P. McGuckin, R. Pettengell, S.M. Watt, Endolyn (CD164) modulates the CXCL12-mediated migration of umbilical cord blood CD133+ cells, Blood 109 (2007) 1825–1833.